Recognition of Single Mismatched DNA Using MutS-Immobilized Carbon Nanotube Field Effect Transistor Devices

ARTICLE *in* THE JOURNAL OF PHYSICAL CHEMISTRY B · SEPTEMBER 2009

Impact Factor: 3.3 · DOI: 10.1021/jp9063559 · Source: PubMed

6 AUTHORS, INCLUDING:

Hye Ryung Byon
RIKEN
36 PUBLICATIONS **1,158** CITATIONS
SEE PROFILE

Hyun-Joon Shin
Pohang University of Science and Technol…
170 PUBLICATIONS **2,655** CITATIONS
SEE PROFILE

Hee Cheul Choi
Pohang University of Science and Technol…
95 PUBLICATIONS **3,276** CITATIONS
SEE PROFILE

THE JOURNAL OF PHYSICAL CHEMISTRY B LETTERS

2009, *113,* 12164–12168
Published on Web 08/17/2009

Recognition of Single Mismatched DNA Using MutS-Immobilized Carbon Nanotube Field Effect Transistor Devices

Suphil Kim,[†] Tae Gyun Kim,[†] Hye Ryung Byon,[†,‡] Hyun-Joon Shin,[§] Changill Ban,*[,†] and Hee Cheul Choi*[,†]

Department of Chemistry and Division of Advanced Materials Science, Pohang University of Science and Technology (POSTECH), Pohang 790-784, South Korea, Department of Mechanical Engineering and Department of Materials Science and Engineering, Massachusetts Institute of Technology (MIT), Cambridge, Massachusetts 02139, and Pohang Accelerator Laboratory (PAL) and Department of Physics, Pohang University of Science and Technology (POSTECH), Pohang 790-784, South Korea

Received: July 6, 2009; Revised Manuscript Received: August 7, 2009

Label-free and real-time detections of mismatched dsDNAs are demonstrated using MutS-protein-immobilized, single-walled carbon nanotube field effect transistor (SWNT-FET) devices. The *E. coli* MutS proteins specifically recognizing mismatched dsDNAs are immobilized on SWNT-FET devices that have been fabricated for high sensitivity using a shadow mask lithographic technique to obtain a thin and wide Schottky contact region. The MutS-immobilized SWNT-FETs have successfully detected 40 base pair dsDNAs having single G-T mismatches at the 20th base pair positions by displaying significant electrical conductance drops at as low as 100 pM concentration. Systematic control experiments have revealed that the signal changes indeed originated from specific recognitions of mismatched DNAs by the immobilized MutS proteins.

Introduction

Numerous human genetic diseases are attributed to small genetic disorders that could be accumulated by abnormal gene duplications and expressions leading to distortion and deletion of gene information. Therefore, early, fast, and reliable detection of genetic damages such as single base replacements, unpaired bases, and insertion and deletion of DNA sequences needs to be established to prevent such potential risks of genetic diseases. MutS protein and its homologues are nature's built-in molecular systems that specifically recognize mismatched double-stranded DNA (dsDNA).[1] Hence, MutS proteins have been considered as a promising probe to detect mismatched dsDNA. The selective capturing of mismatched dsDNA by MutS proteins has been demonstrated in various forms of detection systems, for example, fluorescence,[2] surface plasmon resonance (SPR),[3] quartz crystal microbalance (QCM),[4] electrochemistry,[1d,e,5] and atomic force microscopy (AFM).[6] These techniques have not just evidenced the specific recognitions of mismatched dsDNA by MutS proteins but also successfully provided the details about biochemical information including binding constants between the mismatched dsDNA and MutS proteins, diffusion constants, binding energy differences according to the mismatch types, and so forth. However, it is still challenging to realize a compact sensor system that can detect mismatched dsDNA in a label-free and real-time mode, especially with a low detection limit. The current detection limit of mismatched DNA using a MutS-based sensor is around micromolar level.[5]

Herein, we report a highly selective and sensitive detection of single mismatched dsDNAs in a real-time and label-free detection mode using MutS-immobilized single-walled carbon nanotube field effect transistors (SWNT-FETs). SWNT-FETs have been demonstrated as a potential electrical biosensor platform where the conductance of one-dimensional semiconducting SWNTs is promptly modulated upon specific recognitions of biomolecular interactions occurring from pairs of small molecules−proteins, proteins−proteins, and aptamers−proteins.[7] Moreover, SWNT-FETs provide an opportunity to develop a highly sensitive device by exploiting two main sensing regions, that is (1) the Schottky contact region formed at SWNT and electrode metal contacts and (2) the SWNT channel itself, depending on the electrical charge states of target molecules in sensing media. For example, an instant electrical signal change occurs from a SWNT-FET device when target molecules whose electrical charges are more or less neutral are adsorbed onto the SWNT−metal Schottky region via Schottky barrier modulation.[8] On the contrary, a direct charge (either e^- or h^+) injection from target molecules into SWNT channels (conduction band or valence band) also causes electrical signal changes when significant electrical charges are developed in the target molecules (for example, when the pI of a protein is largely different from the pH of the medium). Recently, we have demonstrated that mat-type SWNT-FET devices of which Schottky contact regions become wider by utilizing a shadow mask fabrication process indeed show a capability to specifically detect less charged target biomolecules at as low as 1 pM concentration, which is about a 4 orders of magnitude increased sensing power compared to the microfabricated mat-type

* To whom correspondence should be addressed. E-mail: choihc@postech.edu (H.C.C.); ciban@postech.edu (C.B.).
[†] Department of Chemistry and Division of Advanced Materials Science, Pohang University of Science and Technology.
[‡] Massachusetts Institute of Technology.
[§] Pohang Accelerator Laboratory (PAL) and Department of Physics, Pohang University of Science and Technology.

10.1021/jp9063559 CCC: $40.75

devices.[8a,b] Since the main target to detect in the current study is mismatched dsDNA, whose negative backbone charges are fairly neutralized with counter cations in a buffer medium, the MutS-immobilized mat-type SWNT-FET devices with increased Schottky region are believed to be suitable for the specific detection of mismatched dsDNA in a real-time and label-free mode.

Experimental Section

Fabrication of Single-Walled Carbon Nanotube Field Effect Transistors (SWNT-FETs). Catalyst islands (2 mm × 2 mm) for the area-selective growth of SWNTs were prepared on a SiO_2/p-Si substrate (SiO_2 thickness = 500 μm) using a conventional photolithography process. Spin-coated photoresist (Az7210) on the substrate was patterned after irradiation of UV light (wavelength = 365 nm) followed by developments. The iron catalyst nanoparticles were then formed inside of the catalyst island pattern area by soaking the substrate in 10 mL of deionized (DI) water where 10 μL of 10 mM $FeCl_3 \cdot 6H_2O$(aq) and 100 μL of 40 mM $NH_2OH \cdot HCl$(aq) were added and incubated for 3 min.[9] After removal of the photoresist using acetone, the SiO_2/Si substrate containing catalyst nanoparticles was brought into a quartz tube, which was then placed in a chemical vapor deposition (CVD) system. SWNTs were grown from the catalysts when H_2 = 500 sccm, CH_4 = 1000 sccm, and C_2H_4 = 16 sccm were introduced at 880 °C for 10 min. Note that before the injection of hydrocarbon gases, the inner atmosphere of the quartz tube was fluently flushed with Ar and H_2 for 5 min, and the temperature was increased under a H_2 atmosphere. Finally, the metal electrodes were deposited using a shadow mask and metal evaporator. The shadow mask template having 2 mm of width and 80 μm of length between two electrodes was settled on the SWNT-grown substrate, and 15 nm of Cr and 25 nm of Au were sequentially deposited using the metal evaporator while the sample substrate was rotated.

Immobilization of *Escherichia coli* (*E. coli*) MutS. The SWNT-FET was incubated in 10 mM of (1*S*)-*N*-[5-[(4-mercaptobutanoyl)amino]-1-1carboxylpentyl] iminodiacetic acid (HS-NTA) for 4 h at room temperature.[10] After washing and drying with N_2 gas, the device was immersed in a 100 mM $NiSO_4$ solution for 1 h and then in 1 μM N-terminal six histidines group-tagged *E. coli* MutS (called His-tagged MutS) for 3 h.[5] The His-tagged MutS/Ni^{2+}/NTA-bound SWNT-FET was thoroughly rinsed with phosphate-buffered saline (PBS, pH 7.4, including 137 mM NaCl/10 mM phosphate buffer/2 mM KCl) solution to remove the unbound proteins.

Preparation of Double-Stranded DNA (dsDNA). Forty base pairs of matched and mismatched dsDNA (Bioneer Inc.) were used. Complementary hybridized DNA pairs consist of the following sequences, 5′-GCA CCT GAC TCC TGT GGA G**A**A GTC GAC GAG CCG CAC GCT A-3′ and 5′-TAG CGT GCG GCT CGT CGA CT**T** CTC CAC AGG AGT CAG GTG C-3′, while single G-T mismatched dsDNA sequences are 5′-GCA CCT GAC TCC TGT GGA G**G**A GTC GAC GAG CCG CAC GCT A-3′ and 5′-TAG CGT GCG GCT CGT CGA CT**T** CTC CAC AGG AGT CAG GTG C-3′.

Ethylenediaminetetraactetic Acid (EDTA) Treatment. The used MutS-immobilized SWNT-FET devices were incubated in a 100 mM EDTA solution for 4 h. To reimmobilize MutS proteins, the EDTA-treated FET devices were immersed in a 100 mM $NiSO_4$ solution for 1 h and then in a 1 μM His-tagged MutS solution for 3 h.

Electrical Measurements. The $I_{DS}-V_G$ characteristic curves of the devices and conductance changes of MutS-immobilized SWNT-FET devices were measured using a semiconductor analyzer (KEITHKEY 4200). For the sensing experiments, the MutS-functionalized SWNT-FET devices were installed into a homemade Teflon electrochemical cell having 1 mm of mouth diameter. The cell was filled with PBS solution where a Pt wire was soaked, and 10 mV of bias voltage (V_{DS}) was applied to the SWNT-FETs.

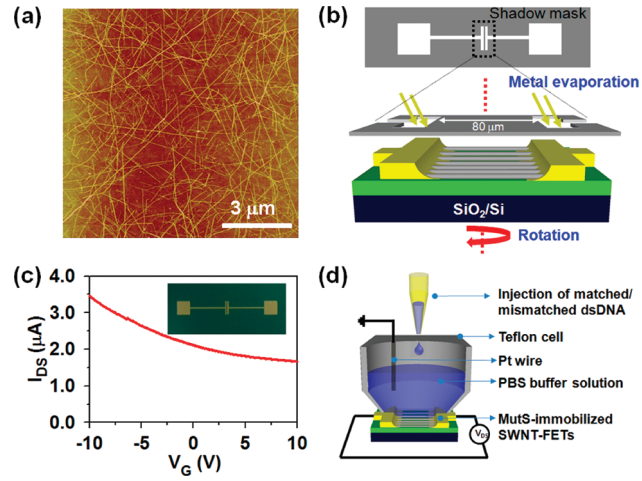

Figure 1. (a) Atomic force microscopy (AFM) image of mat-type SWNTs in the SWNT-FETs. (b) Schematic view of a shadow mask and metal evaporation results for the source and drain electrodes with rotation. (c) Representative $I_{DS}-V_G$ characteristic curve of a SWNT-FET device fabricated using a shadow mask. Inset: optical image shows a real SWNT-FET device used in this experiment (V_{DS} = 10 mV). (d) Scheme of a homemade Teflon electrochemical cell for the electrical sensing.

Results and Discussion

The SWNT-FETs were fabricated on a thermally oxidized p-type Si wafer (SiO_2 thickness = 500 nm), where high-yield mat-type SWNTs were grown by chemical vapor deposition (CVD, Figure 1a).[9] The metal contacts (Au/Cr, thickness = 25/15 nm) for the source and drain metal electrodes were thermally deposited through a homemade Cr-based alloy metal shadow mask (Figure 1b). According to the dimension of the shadow mask, the electrode gap distance is supposed to be 80 μm. However, the actual electrode gap distance becomes much shorter because the evaporated metals passing through the shadow mask also deposit on the regions underneath of the mask due to the naturally formed vertical gap between the substrate and shadow mask. Such SWNT-FETs typically show the on/off < 1 in $I_{DS}-V_G$ curves, signifying the successful formation of thin and wide metal contacts on coexisting mat-type semiconducting and metallic SWNTs (Figure 1c).[8b,c]

The SWNT-FET devices were then assembled into a homemade Teflon electrochemical cell for both immobilization of MutS proteins and sensing of mismatched dsDNA. As shown in Figure 1d, a Teflon reservoir was placed on top of a SWNT-FET device as it secures the exposure of SWNT channels as well as metal-SWNT contact regions to buffer solution containing biomolecules. After rinsing and stabilizing the device with buffer solution, *E. coli* MutS proteins tagged with six histidines at the N-terminal (called His-tagged-MutS) were immobilized on the source and drain Au electrode surfaces via three sequential steps (Figure 2), (a) self-assembly of (1*S*)-*N*-[5-[(4-mercaptobutanoyl)amino]-1-carboxypentyl] iminodiacetic acid (HS-NTA) on the source and drain electrodes, (b) chelation of Ni^{2+} ions to NTA by adding a 100 mM $NiSO_4$ aqueous

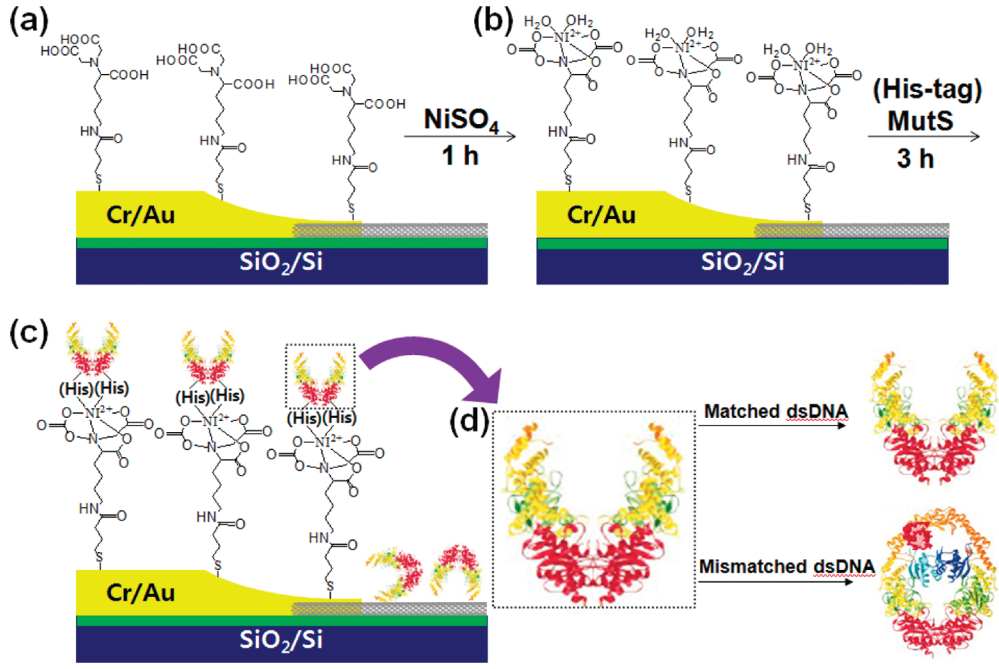

Figure 2. Schematic views of the immobilization of MutS proteins and recognition of dsDNAs on SWNT-FETs. (a) Self-assembly of HS-NTA on a Cr/Au electrode. (b) Chelation of Ni^{2+} ions to NTA. (c) Anchoring of His-tagged-MutS proteins. (d) Active site of MutS proteins to grab mismatched dsDNA and its configuration change after the detection of dsDNA (dsDNA is omitted for clarification).[2b,5]

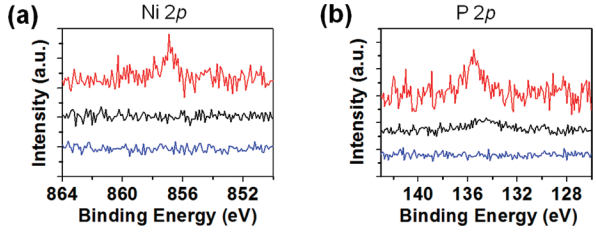

Figure 3. XPS results showing (a) Ni 2p and (b) P 2p peak regions obtained from three control samples, Au (red), bare SWNT (black), and SiO_2/Si (blue) substrates after sequential treatments with NTA, Ni^{2+}, His-tagged MutS, and injection of single G-T mismatched dsDNAs.

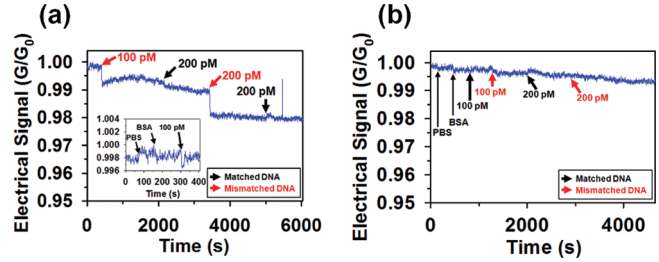

Figure 4. Real-time sensing of mismatched dsDNA. Conductance changes upon the injections of matched (black arrows)/mismatched (red arrows) dsDNAs into the SWNT-FET devices treated with (a) MutS/Ni^{2+}/NTA and (b) Ni^{2+}/NTA, respectively. The concentration denotes the final concentration of the solution after each injection. The inset in (a) shows a magnified view in the region of 0−400 s of graph (a).

solution,[5,10] and finally (c) anchoring histidines of MutS proteins to divalent Ni^{2+} ions with orientation-controlled active sites on the electrodes. Note that all of these steps proceeded in the Teflon electrochemical cell.

The successful functionalizations of HS-NTA and chelation of Ni^{2+} ions were confirmed by monitoring the Ni 2p peak by synchrotron XPS (8A1 beamline, Pohang Accelerator Laboratory, photon energy = 1253.6 eV). For the XPS studies, Au films thermally evaporated on SiO_2/Si substrates (Au/SiO_2/Si), SWNTs grown by CVD on SiO_2/Si substrates (SWNT/SiO_2/Si), as well as pure SiO_2/Si substrates were independently prepared and then sequentially treated with HS-NTA, $NiSO_4$ solution, and MutS proteins. Note that the substrate size was 10×10 mm^2, in which approximately 20 SWNTs/μm^2 with an average length of 5 μm were present. As shown in Figure 3a, the Ni 2p peak corresponding to Ni^{2+} was detected at 856.9 eV from the fully treated Au/SiO_2/Si samples, while this peak was absent from both pure SiO_2/Si and SWNT/SiO_2/Si substrates treated identically. More direct evidence for the MutS protein immobilization was obtained by observing the P 2p peak at 135.5 eV, a signature of phosphate backbones of DNA, after immersing the fully treated (i.e., MutS protein containing) Au/SiO_2/Si samples into a solution of 10 nM of 40 base pairs of dsDNAs having a single G-T mismatch at the 20th base pair position (Figure 3b). On the contrary, the P 2p peak intensities were negligible from SiO_2/Si and SWNT/SiO_2/Si substrates. These results imply that MutS proteins are specifically immobilized on the Au surface through the sequential treatments with highly suppressed nonspecific bindings to SiO_2 or SWNT surfaces and also imply that the immobilized MutS proteins specifically bind mismatched dsDNA.

The real-time electrical sensing of MutS-immobilized SWNT-FETs was performed using a homemade Teflon electrochemical cell which was filled with phosphate-buffered saline (PBS, pH = 7.4). The device was held up until the current level was stabilized under the bias voltage (V_{DS}) of 10 mV applied between the source and drain electrodes. Prior to the detection of mismatched DNA pairs, several aliquots of PBS and 100 pM bovine serum albumin (BSA) solutions were added to test the steady current state and the tolerance to the false electrical signal by nonspecific bindings, respectively. As shown in Figure 4a inset, there was negligible signal modulation upon the injections of PBS and BSA, indicating that the MutS-immobilized SWNT-FET devices are electrically stable and highly resistant to nonspecific adsorptions.

The detection of mismatched DNA was then performed by alternatively injecting perfectly matched and single G-T mis-

matched dsDNA solutions. A significant conductance drop was clearly observed when 100 pM G-T mismatched dsDNA was injected (Figure 4a, red arrow with 100 pM). To verify that this current change was indeed induced by the specific recognition of mismatched dsDNA, 200 pM perfectly matched dsDNA was injected into the same cell. As marked with a black arrow, the device did not respond to the perfectly matched dsDNA with no electrical signal change (Figure 4a, black arrow with 200 pM). Such a test was repeated once again in the same cell, and the results were identical as the device showed another significant conductance drop upon the injection of 200 pM G-T mismatched dsDNA, and no signal change was observed upon the injection of 200 pM perfectly matched dsDNA. Note that the concentration denotes the final concentration of the solution after each injection. To verify the role of MutS proteins on sensing, SWNT-FET devices treated only with HS-NTA and Ni^{2+} chelation without His-tagged MutS proteins were examined as a control experiment. As shown in Figure 4b, when there was no MutS protein, no electrical signal change was observed at all upon the additions of PBS, BSA, and 40 base pairs of matched/mismatched dsDNAs. These results are evident for the electrical sensing of mismatched DNA via specific recognitions by the MutS proteins immobilized on SWNT-FETs.

Our SWNT-FET devices show reliable detection ability to mismatched dsDNAs with an approximately 0.8% conductance drop, which corresponds to >6:1 of signal-to-noise ratio. Moreover, the current detection limit of 100 pM is noteworthy since it is the lowest value among the previously reported real-time mismatched DNA detection by MutS-mediated electrochemical sensing.[5] Such a high sensitivity is attributed to the wide Schottky contact regions responsible for active sensing, on which MutS proteins are highly populated to recognize mismatched dsDNA even at low concentration. Consequently, the origin of the conductance drop upon the recognitions of mismatched dsDNA is believed to be the Schottky barrier modulation, which readily occurs by specific adsorption of mismatched dsDNAs to MutS proteins dominantly deposited on the metal−SWNT contact regions. The possibility of direct charge injection from mismatched dsDNA into SWNT can be ignored because the population of MutS nonspecifically adsorbed on the sidewalls of SWNTs is very low (Figure 5a). This result is also in good agreement with the aforementioned XPS results. To further verify that these nonspecifically adsorbed MutS proteins are not capable of detecting mismatched dsDNA, the electrical detection experiment was performed with SWNT-FET devices containing nonspecifically adsorbed MutS proteins on both metal−SWNT contact regions as well as SWNT surfaces. As shown in Figure 5b, there was no noticeable electrical signal change upon the additions of various matched and mismatched dsDNAs even at higher concentration (1 nM). This result clarifies that MutS proteins strategically immobilized on the device are critically responsible for the sensing of mismatched dsDNA and that the main electrical signal change is induced by the Schottky barrier modulation.

Another advantage of our MutS-immobilized SWNT-FETs is that the MutS-mismatched dsDNA conjugates are easily removed by a simple chemical treatment so that the further investigation into the paired MutS-mismatched dsDNA conjugates would be possible, while the devices become recyclable. After the real-time sensing was finished, the device was treated with a 100 mM EDTA solution to remove MutS-mismatched dsDNA parts still anchored to Ni^{2+} ions from HS-NTA.[5,10] XPS data obtained from the EDTA-treated MutS-immobilized Au substrate show the silencing of both Ni 2p and P 2p peaks, which

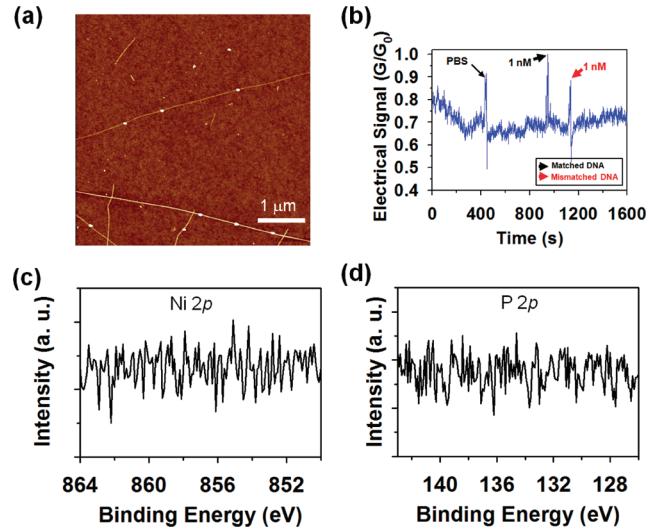

Figure 5. (a) AFM image of SWNTs after treating with 100 nM MutS protein solutions for 2 h. (b) Electrical signal changes upon various treatments from the SWNT-FET device on which MutS proteins are nonspecifically adsorbed. (c,d) XPS results scanned for Ni 2p and P 2p, respectively, from an EDTA-treated Au film, where mismatched dsDNA/MutS/Ni^{2+}/NTA were originally immobilized.

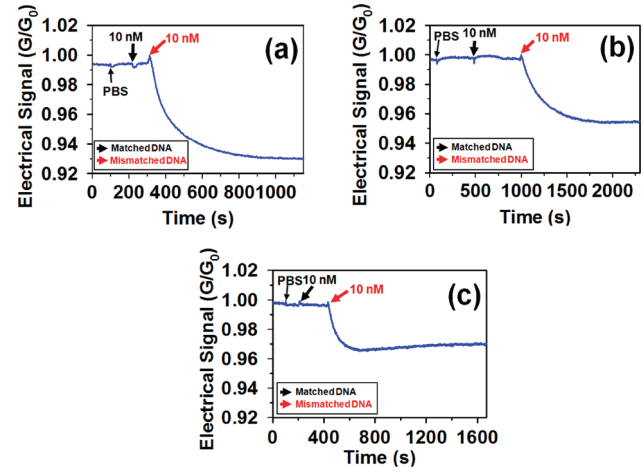

Figure 6. Recycling tests of MutS-immobilized SWNT-FET devices. (a−c) Real-time measurements using a pristine SWNT-FET device, after first recycle, and after second recycle, respectively. The black and red arrows indicate additions of matched and mismatched dsDNAs, respectively.

confirms the successful removal of MutS-mismatched dsDNA conjugates (Figure 5c and d). The device was then retreated with $NiSO_4$ followed by His-tagged-MutS protein solutions to build the device to be reusable. Figure 6 shows the electrical sensing responses to 10 nM matched and mismatched dsDNAs from pristine MutS-immobilized (Figure 6a), first-time recycled (Figure 6b), and second-time recycled (Figure 6c) devices. Note that higher concentrations of DNA solutions were used for clear demonstration. Although the electrical signal change of the recycled device is reduced from 6.6 to 4.5%, the device still shows high selectivity and sensitivity.

Summary

We demonstrated label-free and real-time detections of single mismatched dsDNAs at picomolar concentration level using MutS-immobilized SWNT-FETs. In contrast to the conventional SWNT-FET DNA sensors operated by the signal induction upon hybridizations between specific base sequences of probe and

target single-stranded DNAs (ssDNAs),[8c,d,11] the use of mismatched dsDNA-specific probe proteins is beneficial to a variety of base pairs of dsDNAs without a restriction of probe. The MutS-immobilized SWNT-FET is further expected to provide an ideal platform for the sophisticated investigation of relative binding affinities between MutS proteins and various possible mismatches, such as C-T, T-T, C-C, and A-T.

Acknowledgment. This work was supported by the Nano/Bio Science & Technology Program of MEST (2005-01325), KOSEF through the EPB center (R11-2008-052-02001-0), KOSEF (2008-04306, 2007-8-1158), and the Korean Research Foundation (KRF-2005-005-J13103). H.C.C. thanks to the World Class University (WCU) program (R31-2008-000-10059-0).

References and Notes

(1) (a) Lu, A. L.; Clark, S.; Modrich, P. *Proc. Natl. Acad. Sci. U.S.A.* **1983**, *80*, 4639. (b) Lieb, M. *J. Bacteriol.* **1987**, *169*, 5241. (c) Schofield, M. J.; Hsieh, P. *Annu. Rev. Microbiol.* **2003**, *57*, 579. (d) Han, A.; Shibata, T.; Takarada, T.; Maeda, M. *Nucleic Acids Res. Suppl.* **2002**, *2*, 287. (e) Li, C.-Z.; Long, Y.-T.; Lee, J. S.; Kraatz, H.-B. *Chem. Commun.* **2004**, *5*, 574.

(2) (a) Behrensdorf, H. A.; Pignot, M.; Windhab, N.; Kappel, A. *Nucleic Acids Res.* **2002**, *30*, e64. (b) Cho, M.; Chung, S.; Heo, S.-D.; Ku, J.; Ban, C. *Biosens. Bioelectron.* **2007**, *22*, 1376.

(3) (a) Gotoh, M.; Hasebe, M.; Ohira, T.; Hasegawa, Y.; Shinohara, Y.; Sota, H.; Nakao, J.; Tosu, M. *Genet. Anal.* **1997**, *14*, 47. (b) Babic, I.; Andrew, S. E.; Firik, F. R. *Mutat. Res.* **1996**, *372*, 87.

(4) Su, X.; Robelek, R.; Wu, Y.; Wang, G.; Knoll, W. *Anal. Chem.* **2005**, *76*, 489.

(5) Cho, M.; Lee, S.; Han, S.-Y.; Park, J.-Y.; Rahman, M. A.; Shim, Y.-B.; Ban, C. *Nucleic Acids Res.* **2006**, *34*, e75.

(6) (a) Wang, H.; Yang, Y.; Schofield, M. J.; Du, C.; Fridman, Y.; Lee, S. D.; Larson, E. D.; Drummond, J. T.; Alani, E.; Hsieh, P.; Erie, D. A. *Proc. Natl. Acad. Sci. U.S.A.* **2003**, *100*, 14822. (b) Sun, H. B.; Yokota, H. *Anal. Chem.* **2000**, *72*, 3138.

(7) (a) Besteman, K.; Lee, J.-O.; Wiertz, F. G. M.; Heering, H. A.; Dekker, C. *Nano Lett.* **2003**, *3*, 727. (b) Chen, R. J.; Bangsaruntip, S.; Drouvalakis, K. A.; Kam, N. W. S.; Shim, M.; Li, Y.; Kim, W.; Utz, P. J.; Dai, H. *Proc. Natl. Acad. Sci. U.S.A.* **2003**, *100*, 4984. (c) Star, A.; Gabriel, J.-C. P.; Bradley, K.; Gruner, G. *Nano Lett.* **2003**, *3*, 459. (d) Li, C.; Curreli, M.; Lin, H.; Lei, B.; Ishikawa, F. N.; Datar, R.; Cote, R. J.; Thompson, M. E.; Zhou, C. *J. Am. Chem. Soc.* **2005**, *127*, 12484. (e) So, H.-M.; Won, K.; Kim, Y. H.; Kim, B.-K.; Ryu, B. H.; Na, P. S.; Kim, H.; Lee, J.-O. *J. Am. Chem. Soc.* **2005**, *127*, 11906. (f) Wang, C.-W.; Pan, C.-Y.; Wu, H.-C.; Shih, P.-Y.; Tsai, C.-C.; Liao, K.-T.; Lu, L.-L.; Hsieh, W.-H.; Chen, C.-D.; Chen, Y.-T. *Small* **2007**, *3*, 1350.

(8) (a) Chen, R. J.; Choi, H. C.; Bangsaruntip, S.; Yenilmez, E.; Tang, X.; Wang, Q.; Chang, Y.-L.; Dai, H. *J. Am. Chem. Soc.* **2004**, *126*, 1563. (b) Byon, H. R.; Choi, H. C. *J. Am. Chem. Soc.* **2006**, *128*, 2188. (c) Tang, X.; Bansaruntip, S.; Nakayama, N.; Yenilmez, E.; Chang, Y.-I.; Wang, Q. *Nano Lett.* **2006**, *6*, 1632. (d) Gui, E. L.; Li, L.-J.; Zhang, K.; Xu, Y.; Dong, X.; Ho, X.; Lee, P. S.; Kasim, J.; Shen, Z. X.; Rogers, J. A.; Mhaisalkar, S. G. *J. Am. Chem. Soc.* **2007**, *129*, 14427.

(9) Choi, H. C.; Kundaria, S.; Wang, D. W.; Javey, A.; Wang, Q.; Rolandi, M.; Dai, H. *Nano Lett.* **2003**, *3*, 157.

(10) Roure, O. Du.; Debiemme-Chouvy, C.; Malthête, J.; Silberzan, P. *Langmuir* **2003**, *19*, 4138.

(11) (a) Star, A.; Tu, E.; Niemann, J.; Gabriel, J.-C. P.; Joiner, C. S.; Valcke, C. *Proc. Natl. Acad. Sci. U.S.A.* **2006**, *103*, 921. (b) Tang, X.; Bansaruntip, S.; Nakayama, N.; Yenilmez, E.; Chang, Y.-I.; Wang, Q. *Nano Lett.* **2006**, *6*, 1632. (c) Dong, X.; Lau, C. M.; Lohani, A.; Mhaisalkar, S. G.; Kasim, J.; Shen, Z.; Ho, X.; Rogers, J. A.; Li, L.-J. *Adv. Mater.* **2008**, *20*, 2389.

JP9063559